COMPARISON OF EULER AND MODIFIED TSP SOLUTIONS FOR UNSTEADY TRANSONIC FLOW CALCULATIONS

Rajesh Kumar* and Navtej Singh**

Abstract

Many prediction methods have been developed for the transonic flow calculations, most of them solve the Euler equations. The solution of Euler equations is usually complex and takes long computer time. However, in many practical applications, viz, flutter calculation faster transonic flow calculation is preferred. One such approach is based on modified transonic small perturbation (TSP) theory approach. Here in this paper modified TSP theory incorporating entropy and vorticity effects has been studied by comparing the results with those of Euler equations. The paper presents the description of both the Euler solver and the TSP solver incorporating entropy vorticity effects. The calculated results have been compared with the available experimental results or with available Euler results from literatures. The comparison shows good agreement with the experimental data as well as available data from open literature. The modified TSP code provides acceptable accuracy for most transonic flow calculations. Thus in most cases long computation involved in Euler code can be avoided.

Nomenclature

a	speed of sound
e	total energy per unit volume
C_p	pressure coefficient
F,G,H	flux vectors
$H^{\pm}$	forward and backward component of flux vector
I	identity matrix
k	reduced frequency, $\omega c_r/2U$
M	Mach number
p	pressure
q_{ij},q_{ik}	vectors of primitive variables at the centroids of cell i,j and i,k
Q	conserved variables
s	flux limiter
S_{ij}	cell area
Δs	length of cell side
Δt	time step
u, v	cartesian velocity components
U, V	conservative variables
x, y	cartesian coordinates to local normal/tangential coordinates
x_t, y_t	grid speed in the x and y directions
$\Delta x,\Delta y$	directed lengths of the edge in x and y directions
α,α_0,α_1	instantaneous angle, mean angle of attack, and amplitude of pitch oscillation
Γ	circulation
γ	ratio of specific heats
ε	very small number
ρ	density
Φ	flux function

Introduction

Considerable progress has been made over the past few decades in developing methods for aeroelastic analysis in the flutter critical transonic speed range [1-10]. Much of this progress has been achieved by developing finite-difference computer codes for solving transonic small perturbation (TSP) potential equation, although significant efforts are currently underway at the higher equation levels as well. The advantages of the TSP formulation, especially for aeroelastic applications, are the relatively low computational cost and the simplicity involving the grid and geometry preprocessing. However, a serious limitation of the potential flow codes, in general, is the inability to predict accurately flows with strong shock waves. For such flows, use of the isentropic potential formulation

* Research Scholar ** Associate Professor
Department of Aerospace Engineering, Indian Institute of Technology Kharagpur, Kharagpur-721 302, India
Email : rajesh@aero.iitkgp.ernet.in; nsingh@aero.iitkgp.ermet.in
Manuscript received on 02 Aug 2005; Paper reviewed, revised and accepted on 07 Oct 2005

typically results in shock waves that are too strong and located too far aft in comparison with the experiment. In fact, it is fairly well known that the potential theory predicts non-unique steady-state solutions [2] for certain combinations of Mach number and angle of attack. Simple modifications to potential theory [6-10], however, have been shown to eliminate the non-uniqueness problem and, consequently, provide solutions that more accurately simulate those computed using the Euler equations. These modifications include the effects of shock-generated entropy, and they require only minor changes to existing computer codes.

Rotational effects may also become important when strong shock waves are present in the flow. For example, vorticity is generated by shock waves due to the variation of entropy along the shock. Potential theory, of course, does not account for these effects because of the irrotationality assumption necessary for the existence of a velocity potential. For such flows, the Euler equations generally are required to model the flow accurately. However, simple modifications to potential flow theory have been developed to model rotational effects [8-10]. These modifications involve velocity decomposition. In this model, the velocity vector is decomposed into a potential component and a rotational component. For most applications of interest to the aeroelastician, the rotational effects are significant only in the region downstream of shocks. Therefore, the potential component can be obtained throughout most of the flow field using an existing potential flow code. The rotational flow then can be modeled either by adding the appropriate source term to the governing equation or by modifying the fluxes. These changes, consequently, include the effects of the shock-generated vorticity as well as entropy, and require relatively straightforward modifications to existing potential flow codes.

Euler solver has also been developed, to solve the time-dependent compressible Euler equations using structured dynamic mesh for time-accurate unsteady flow applications. The driving algorithm is an upwind biased implicit cell-centered finite volume scheme. The spatial discretization involves naturally dissipative flux-vector split approach of Van Leer [11] that sharply captures shockwaves.

The purpose of this paper is to study the entropy and the vorticity corrections to TSP equation in comparison with Euler solver. The computed results for steady and unsteady cases obtained by these two models have been compared with each other, with available experimental data and also with Euler solutions available in the literature, which assess the accuracy of the developed codes and their applicability.

Euler Algorithm

The flow is assumed to be governed by the two-dimensional unsteady Euler equations for a bounded domain Ω with a boundary $\partial\Omega$ that may be written in integral form as;

$$\frac{\partial}{\partial t}\int_{\Omega}\int Q dx dy + \int_{\partial\Omega}(F dy - G dx) = 0 \tag{1}$$

where the vector of conserved variables Q and the convective fluxes F and G are given by

$$Q = \begin{pmatrix} \rho \\ \rho u \\ \rho v \\ e \end{pmatrix},\quad F = \begin{pmatrix} \rho U \\ \rho U u + p \\ \rho U v \\ (e+p)\,U + x_t p \end{pmatrix},\quad G = \begin{pmatrix} \rho V \\ \rho V u \\ \rho V v + p \\ (e+p)\,V + y_t p \end{pmatrix}$$

The contravariant velocities U and V are defined by

$$U = u - x_t \qquad V = u - y_t \tag{2}$$

where x_t and y_t are the grid speeds in the x and y directions, and are obtained from the grid movement algorithm, respectively, and the pressure p is given by the equation of state for a perfect gas

$$p = (\gamma - 1)\left[e - \tfrac{1}{2}\rho(u^2 + v^2)\right] \tag{3}$$

Flux-Vector Splitting

The inviscid fluxes computed using finite volume method, cell-centered upwind flux-vector splitting (FVS) scheme of Van Leer [11]. In this method the flux vectors are split into forward and backward contributions, which are continuously differentiable even at sonic and stagnation points. The scheme is derived as follows.

For each edge of a cell, the fluxes are first rotated into a locally Cartesian coordinate system $\bar{x} - \bar{y}$ with the principal direction being perpendicular to the edge. The flux in this direction is defined as,

$$H\Delta s = T(F\Delta y - G\Delta x) = \begin{Bmatrix} \rho\bar{U} \\ \rho\bar{U}\bar{u} + p \\ \rho\bar{U}\bar{v} \\ e\bar{U} + p\bar{u} \end{Bmatrix} \Delta s \tag{4}$$

where T is the transformation matrix, Δx and Δy are the directed lengths of the edge in the x and y coordinate directions, respectively, and $\Delta s^2 = \Delta x^2 + \Delta y^2$. Also, $\bar{u},\bar{v}$ are the Cartesian velocity components perpendicular and parallel to the edge and $\bar{U},\bar{V}$ are the corresponding contravariant velocities.

The flux vector H is split into forward (H^+) and backward (H^-) vectors components.

For locally subsonic flow, at

$$|\bar{U}| < a \quad H = H^+ + H^- \tag{5}$$

where

$$H^{\pm} = \begin{Bmatrix} h^{\pm}_{mass} \\ h^{\pm}_{mass}\left[\dfrac{(-\bar{U} \pm 2a)}{\gamma} + \bar{u}\right] \\ h^{\pm}_{mass}\bar{v} \\ h^{\pm}_{energy} \end{Bmatrix}$$

and $h^{\pm}_{mass}$, $h^{\pm}_{energy}$ taken same as Batina [12].

For locally supersonic flow $|\bar{U}| \geq a$,

For $\bar{U} \geq a \quad H^+ = H, \; H^- = 0$ and for
$\bar{U} \leq -a \quad H^+ = 0, \; H^- = H$

The resulting split fluxes are finally rotated back into the original coordinate system so that

$$F\Delta y - G\Delta x = T^{-1}\left[H^+(q^-) + H^-(q^+)\right]\Delta s \tag{6}$$

where the notation $H^+(q^-)$ and $H^-(q^+)$ indicates that the fluxes $H^{\pm}$ are evaluated by MUSCL type approach, i.e. using upwind-biased interpolations of the primitive variables q. For a given cell (i,j) the upwind-biased interpolation for q^- along the edge between cells (i,j) and (i+1,j) is defined by

$$q^- = q_{i,j} + \frac{1}{4}\left[(1-\mu)\,\delta_- + (1+\mu)\,\delta_+\right]_{i,j} \tag{7}$$

where

$$\delta_+ = q_{i+1,j} - q_{i,j}\,, \quad \delta_- = q_{i,j} - q_{i-1,j} \tag{8}$$

In Equations (7) and (8), $q_{i-1,j}$ $q_{i,j}$ and $q_{i+1,j}$ are the vectors of primitive variables at the centroids of the cells (i-1,j) (i,j) and (i+1,j) respectively. The upwind-biased interpolation for q^+ along this edge is determined similarly using the flow variables at centroids of the cells (i,j) (i+1,j) and (i+2,j), respectively. The parameter μ in the Equation (7) controls a family of difference schemes by appropriately weighting δ_+ and δ_-. In the present calculation μ= 1/3 is used which leads to a third order accurate upwind-biased scheme. Furthermore, in calculations involving upwind-biased schemes, oscillations in the solution near shock waves are expected to occur. To eliminate these oscillations flux limiting is usually required which modifies the upwind-biased interpolations for q^+ and q^- such that,

$$q^- = q_{i,j} + \frac{s}{4}\left[(1-\mu s)\,\delta_- + (1+\mu s)\delta_+\right]_{i,j} \tag{9}$$

where s is the flux limiter [13] given by

$$s = \frac{2\delta_-\delta_+ + \varepsilon}{\delta_-^2 + \delta_+^2 + \varepsilon} \tag{10}$$

where $\varepsilon = 10^{-8}$ is used, a very small number used to avoid division by zero.

Implicit Time-step Integration

The implicit relaxation algorithm is formulated by the first approximating the time derivative in Euler equations by

$$\frac{\partial Q}{\partial t} = \frac{2+\varphi}{2}\frac{\Delta Q}{\Delta t} - \frac{\varphi}{2}\frac{Q^n - Q^{n-1}}{\Delta t} \tag{11}$$

where $\Delta q = Q^{n+1} - Q^n$ and the parameter φ controls the order of temporal accuracy. In the present calculations φ is taken as 1, which gives second order accuracy in time. The flux H must be treated at time level (n+1), which is accomplished by linearizing as,

$$H^{n+1} = H^n + \left(\frac{\partial H}{\partial Q}\right)_{Q=Q^n} \Delta Q \qquad (12)$$

where $\partial H/\partial Q$ is the flux Jacobean A. This linearization, however, reduces the temporal order of accuracy and imposes some stability restrictions. This linearization and relaxation errors can be minimized by, performing sub-iterations to drive to Q^n to Q^{n+1}. The forward and backward fluxes are linearised for a given cell (i,j) as

$$\sum T^{-1}\left[H^+(q^-) + H^-(q^+)\right]^{n+1} \Delta s$$
$$= \sum T^{-1}\left[H^+(q^-) + H^-(q^+)\right]^{n} \Delta s$$
$$+ \left[\sum T^{-1} A^+ \Delta s\right] \Delta Q_{i,j} + \sum_{m=1}^{4} T^{-1} A^- \Delta s \, \Delta Q_m \qquad (13)$$

In this equation ΔQ_m is the change in the flow variables in the cells adjacent to cell (i,j). The exact Jacobians A^+ and A^- are determined by differentiation of H^+ and H^- by conserved variables Q. By combining Equations (11) and (13), the Euler equations are discretized as,

$$\left[\frac{1}{2}(2+\varphi)\left(\frac{S_{i,j}}{\Delta t}\right) I + \sum T^{-1} A^+ \Delta s\right] \Delta Q_{i,j} + \sum_{m=1}^{4} T^{-1} A^- \Delta s \Delta Q_m$$
$$= \frac{1}{2}\varphi S_{i,j} \frac{(Q^n - Q^{n+1})}{\Delta t} - \sum T^{-1}\left[H^+(q^-) + H^-(q^+)\right]^n \Delta s \qquad (14)$$

where I is the identity matrix and $S_{i,j}$ is the area of cell (i,j).

If the discritized equation given above is applied to each cell in the mesh then direct solution of the resulting system of simultaneously equations requires the inversion of a large matrix, even through sparse, with large bandwidth and is enormously expensive. Consequently, a Gauss-Seidel relaxation approach is used in which the summation involving the variables in the neighboring cells ΔQ_m is moved to the right hand side of the Equation (14). The terms in this summation are then evaluated by using the most recent values of ΔQ_m. The solution procedure then involves only the inversion of a 4 x 4 matrix for each cell in the mesh. Solution is obtained by sweeping twice through the mesh. The first sweep is performed in the direction from upstream to downstream and the second sweep is from downstream to upstream.

Boundary Conditions

To impose the flow tangency condition along the surface of airfoil, the flow variables are set within dummy cells that are effectively inside the geometry being considered. The velocity components within the dummy cell are determined from the values in the cell that is adjacent to the surface by requiring the normal velocity component be zero. Also, pressure and density within the dummy cell are set equal to the values in the adjacent cell.

In the far-field [14], a characteristic analysis based on Riemann invariants is used to determine the values of the flow variables on the outer boundary of the grid. This analysis correctly accounts for wave propagation in the far field, which is important for rapid convergence to steady state and serves as a "nonreflecting" boundary condition for unsteady applications.

Computational Grid and Grid Movement Algorithm

A two-dimensional body-fitted curvilinear O-type grid with suitable grid clustering has been generated by solving an elliptic system of second order partial differential equations.

For unsteady calculations, gird movement algorithm have been implemented in which, the grid is moved to conform to the instantaneous position of the body by modeling each edge of each cell by a spring. The spring stiffness (k) of an edge is taken as the reciprocal of the length of the edge concerned. The instantaneous location of the points of the body, the inner boundary is obtained by the prescribed unsteady motion of the body surface and the points on the outer boundary are held fixed. At each time step the displacements of the interior grid points are then solved iteratively using the static equilibrium equations at each node, resulting in a smooth movement of the mesh as the body moves or deforms. From the displacements so found, the new location of the nodes and other grid parameters are obtained readily.

Modified Transonic Small Perturbation Algorithm

The flow is assumed to be governed by the general-frequency TSP potential equation, which maybe written in conservation law form as

$$\frac{\partial f_0}{\partial t} + \frac{\partial f_1}{\partial x} + \frac{\partial f_2}{\partial z} = 0 \tag{15}$$

where

$$f_0 = -A\phi_t - B\phi_x \tag{16a}$$

$$f_1 = E\phi_x + F\phi_x^2 \tag{16b}$$

$$f_2 = \phi_z \tag{16c}$$

The coefficient A, B, E and F are defined as given in reference [4].

The lifting surfaces are modeled by imposing the following conditions:

Flow tangency:

$$\phi_z^{\pm} = f_x^{\pm} + f_t \tag{17a}$$

Trailing wake :

$$\Gamma_t + \Gamma_x = 0 \quad \text{and} \quad \Delta\phi_z = 0 \tag{17b}$$

where $\Delta(\ )$ represents the jump in $(\ )$ across the wake. The flow-tangency condition is imposed along the mean plane of the respective lifting surface. In Equation (17a), the plus and minus superscripts indicate the upper and lower sides of the chord line, respectively. The wake is assumed to be a planar extension from the trailing edge to the downstream boundary of the finite-difference grid.

Entropy Model

Shock-generated entropy is modeled by implementing modifications to TSP theory [6,7]. These modifications include; an alternative stream wise flux, an entropy correction in the pressure formula and a modified wake boundary condition for convection of entropy.

The entropy model is formulated by first replacing the stream-wise flux f_1 in the TSP equation by an alternative flux given by

$$f_1 = (\gamma + 1)\, M^2\, R(V\bar{V} - 1/2V^2) \tag{18}$$

The first term of this new flux was derived [6] by an asymptotic expansion of the Euler equations including the effects of shock-generated entropy.The pressure formula is modified to include entropy effects according to,

$$C_p = C_{pi} + C_{ps} \tag{19}$$

where C_{pi} is the isentropic pressure coefficient, and C_{ps} is the pressure coefficient due to change of entropy and is given by

$$C_{ps} = \frac{-2.S}{\gamma(\gamma - 1)\, M^2 C_v} \tag{20}$$

Equation (20) obviously requires the determination of entropy along the surface of the airfoil. This first requires the determination of the shock location and then the calculation of the entropy jump across the shock. The shock location is determined easily since most TSP algorithms use type-dependent differencing to capture shocks and to treat regions of subsonic and supersonic flow properly. The entropy jump is computed using the Rankine-Hugoniot shock jump relation as,

$$\frac{S}{C_v} = 1n\frac{(\gamma + 1)\, u_1^2 - (\gamma - 1)\, R^2}{(\gamma + 1)\, R^2 - (\gamma - 1)\, u_1^2} - \gamma\, 1n\frac{u_1^2}{R^2} \tag{21}$$

where

$$u_1 = 1 + \phi_x - u_s \tag{22}$$

In Equation (22), u_1 is the flow speed upstream of the shock and u_s is the shock speed, which is computed at time lever (n+1) to maintain time accuracy. In reference [6,7] the entropy was assumed to be constant between the shock and the trailing edge even for unsteady applications. In the present formulation, the entropy is convected downstream from the shock according to,

$$\frac{\partial s}{\partial t} + \frac{\partial s}{\partial x} = 0 \tag{23}$$

The wake boundary condition requires that the pressure be continuous across the wake. Since the pressure formula Equation (19), includes a term due to entropy, the isentropic wake boundary condition must be modified as

$$\Gamma_t + \Gamma_x = 1/2\, \Delta C_{ps} \tag{24}$$

where Δ represents the jump across the wake. In Equation (24), ΔC_{ps} is determined by first convecting the entropy along the wake and then computing C_{ps} using Equation (20). The nonzero right-hand side of Equation (24) modifies the circulation distribution Γ. Consequently, the circulation due to entropy opposes the circulation associated with lift and thus decreases the total circulation. This is the feedback mechanism that stabilizes the shock location and eliminates the non-uniqueness problem [7].

Vorticity Model

The vorticity model modification [8] includes: a modified velocity vector that in turn modifies the TSP equation, a pressure formula correction for vorticity effects, and the resulting wake boundary condition.

The vorticity model is formulated by first writing the velocity vector as the sum of potential and rotational components according to

$$V = \nabla\Phi - \frac{1}{\gamma - 1}\,\frac{s}{C_v}\nabla\psi \tag{25}$$

In Equation (25), the first term on the right-hand side is the gradient of a scalar potential Φ, and the second term involves the product of the entropy s and the gradient of a Clebsch variable ψ. The function ψ is the measure of the stretching and rotating of vortex filaments associated with entropy variation [8]. For the applications of interest in the present work, the rotational part of the velocity vector is assumed to occur only in the region downstream of the shock waves, as shown in Fig.A.

Further assuming that the entropy convects with the free stream speed Equation (23) and that the shock curvature is negligible [8] implies that

$$\frac{\partial\psi}{\partial x} = \frac{1}{\gamma M^2}, \quad \text{and} \quad \frac{\partial\psi}{\partial z} = 0 \tag{26}$$

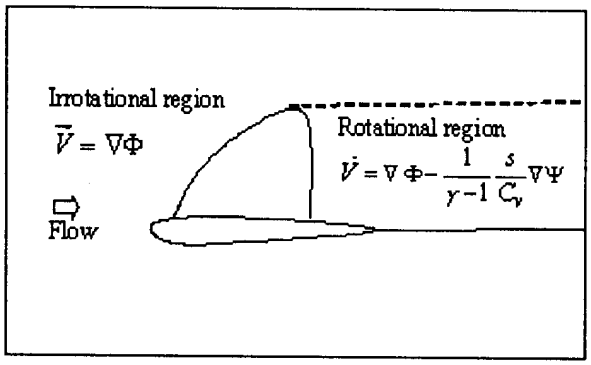

Fig. A Rotational and irrotational flow regions

These assumptions eliminate the variable ψ from the formulation, leaving only the entropy s to be determined throughout the flow field. In a steady flow, entropy is constant along streamlines and changes only through shock waves. The entropy jump is computed along shocks using the Rankine-Hugoniot relation Equation (21). The modified velocity vector in turn modifies the TSP equation because the stream-wise distribution speed $u = \phi_x$ is now given by

$$u = \phi_x - \frac{1}{\gamma(\gamma - 1)\, M^2}\,\frac{s}{c_v} \tag{27}$$

The pressure formula must also be modified when vorticity effects are included in the model. In general form, the pressure coefficient may be computed using

$$C_p = C_{pi} + C_{ps} + C_{pv} \tag{28}$$

where C_{pv} is the pressure coefficient correction due to vorticity. As discussed by Hafez and Lovell [9], the correction due to vorticity approximately cancels the correction due to entropy and, thus, C_p is given by the isentropic formula in terms of the irrotational disturbance speed ϕ_x. As the pressure is now given by isentropic formula, the wake boundary condition is identical to the original condition given by Equation (17b). The feedback mechanism that eliminates the non-uniqueness problem is the rotational velocity field inherent in the vorticity model. This is in contrast to the mechanism of the entropy model, which is explicitly imposed through the wake boundary condition Equation (24).

Approximate Factorization Algorithm

The approximate factorization (AF) algorithm [4] has been modified to solve the TSP equation including entropy and vorticity effects. It consists of a Newton linearization procedure coupled with an internal iteration technique.

For unsteady flow calculations, the solution procedure involves two steps. First, a time linearization step is performed to determine an estimate of the potential field. Second, internal iterations are performed to minimize linearization and factorization errors. Specifically, the TSP equation is written in general form as

$$R(\phi^{n+1}) = 0 \tag{29}$$

where ϕ^{n+1} represents the unknown potential field at time level (n+1). The solution to Equation (29) is then given by the Newton linearization of Equation (29) about ϕ^*

$$R(\phi^*) + \left(\frac{\partial R}{\partial \phi}\right)_{\phi=\phi^*} \Delta\phi = 0 \tag{30}$$

In Equation (30), ϕ^* is the currently available value of ϕ^{n+1} and $\Delta\phi = \phi^{n+1} - \phi^*$. During convergence of the iteration procedure, $\Delta\phi$ will approach zero so that the solution will be given by $\phi^{n+1} = \phi^*$. In general, only one or two iterations are required to achieve acceptable convergence.

The AF algorithm is formulated by first approximating the time derivative terms (ϕ_{tt} and ϕ_{xt}) by second-order accurate finite-difference formulas. The TSP equation is rewritten by substituting $\phi = \phi^* + \Delta\phi$ and neglecting squares of derivatives of $\Delta\phi$, which is equivalent to applying Equation (30) term by term. The resulting equation is then rearranged, and the left-hand side is approximately factored into a triple product of operators, yielding

$$L_x L_z \Delta\phi = -\sigma R\left(\phi^*, \phi^n, \phi^{n-1}, \phi^{n-2},\right) \tag{31}$$

where L_x, L_z and residue R same as [4], σ is a relaxation parameter. Equation (31) is solved using two sweeps through the grid by sequentially applying the operators L_x and L_z as,

x sweep : $L_x \Delta\bar{\phi} = -\sigma R$

z sweep : $L_z \Delta\phi = \Delta\bar{\phi}$

Results and Discussions

To assess the entropy and vorticity modifications to TSP formulation in comparison with the Euler solutions, results are presented for the NACA 0012 airfoil and RAE 2822 transonic airfoil. The accuracy of these results is determined through detailed comparisons with available experimental data. Euler calculations were performed on an O-type structured dynamic grid with 128 x 30 grid points and modified TSP calculations were performed on a grid that had 105 and 45 points in the stream-wise and vertical directions, respectively. For one particular case the Euler results were also obtained by finer grids of size 128 x 50 and 200 x 50 to study the grid consistency as shown in Fig.1. It shows that except for a small difference in the shock strength as obtained by 200 x 50 grid, the three results are identical. Because of considerable time saving 128 x 30 grid is used for all other calculations presented in this paper.

For the NACA 0012 airfoil, four cases of increasing difficulty were selected to assess the accuracy of the modified TSP code in comparison with the Euler solutions systematically. The first two cases involve steady flow for non-lifting (M = 0.85, $\alpha_0 = 0°$) and lifting (M = 0.8, α_0 = 1.25°) conditions. The third case is for the airfoil pitching harmonically about the quarter-chord with an amplitude of α_1 = 2.51° and reduced frequency of k = 0.0814 at M = 0.755 and α_0 = 0.016°. The calculations are compared with the experimental data [13]. This case is a challenging one for the modified TSP code since the oscillating airfoil produces relatively large shock motions and the upper and lower surface shocks periodically appear and disappear

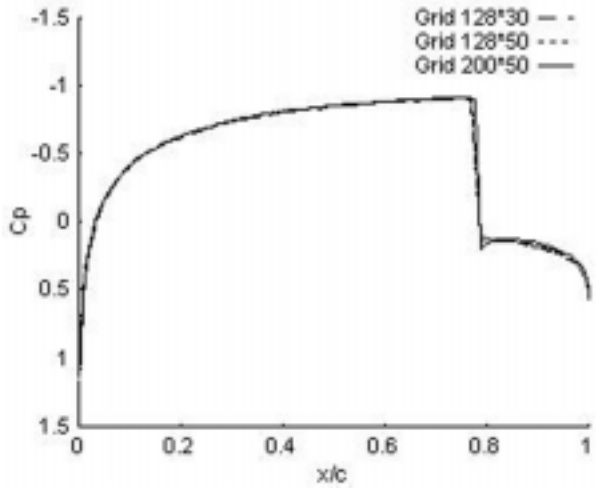

Fig.1 Grid consistency check

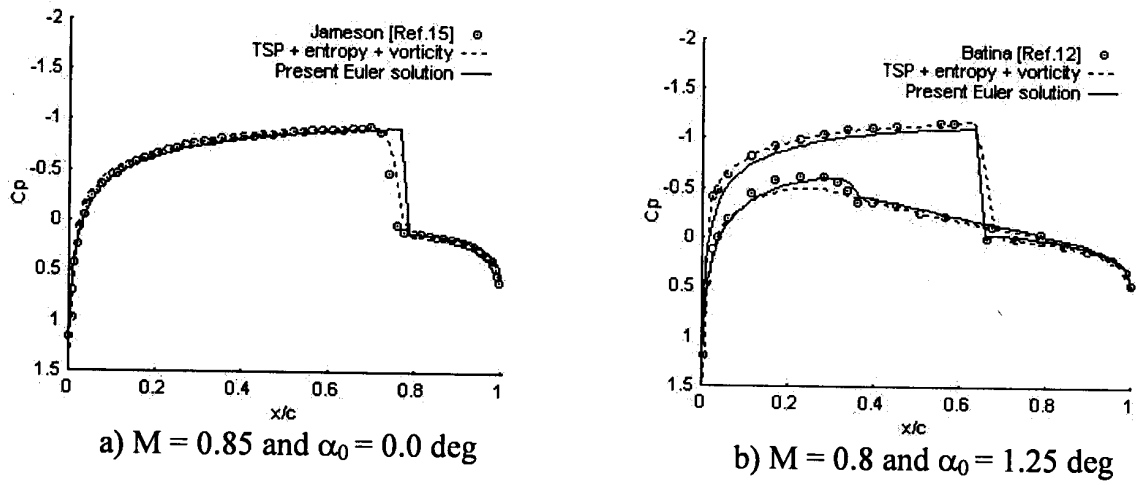

Fig.2 Comparison of steady pressure distributions for NACA 0012 airfoil

during the cycle. The fourth case is for the airfoil pitching harmonically about the quarter-chord with an amplitude of $\alpha_1 = 2.44°$ and reduced frequency of $k = 0.081$ at M = 0.599 and $\alpha_0 = 4.86°$. This case is also a very challenging one since the maximum angle of attack during a cycle of motion is 7.3°. This relatively large instantaneous angle of attack is normally considered to be outside the range of validity of TSP theory. Also result for steady case is presented for RAE 2822 transonic airfoil and comparison were made with experimental data [16].

Steady Flow : Results are first presented for the NACA 0012 airfoil non-lifting flow at M = 0.85 and $\alpha_0 = 0°$. At this Mach number and angle of attack, irrotational isentropic methods, either TSP or full potential, predict non-unique solutions. These non-unique or multiple solutions are characterized by stable asymmetric flows with either large positive or negative lift. The correct solution, of course, is a symmetric flow with zero lift. When shock-generated entropy effects are included in the calculation as a modification to the stream-wise flux, the non-uniqueness problem is eliminated, and the expected symmetric solution is obtained, as show in Fig 2(a). For nonzero lifting case results obtained for M = 0.8, $\alpha_0 = 1.25°$ is presented in Fig 2(b). It is a well studied case in AGARD test cases for assessment of invisicid-flow methods. Obtained results are in good agreement with the experimental data. However, TSP results are unable to capture the weak shock on the lower surface of airfoil whereas Euler solver is capable of capturing it quite accurately. Also, to assess the applicability of the developed algorithms, calculation was performed on RAE 2822 airfoil for M = 0.729 and $\alpha_0 = 2.31°$ and comparison made with experimental data. As shown in Fig 3, an Euler solver result matches well with the experimental data whereas there are small discrepancies in the modified TSP results in terms of shock location and strength.

Unsteady Flow : To assess the modified theory for unsteady flow applications, results obtained for the NACA 0012 airfoil pitching harmonically about quarter chord at M= 0.755 and $\alpha_0 = 0.016°$. The amplitude of the motion selected as $\alpha_1 = 2.51°$ and the reduced frequency k = 0.0814 for comparison with the experimental data. The oscillatory motion is defined by $\alpha = \alpha_0 + \alpha_1 \sin(\omega t)$. The results obtained using 360 steps per cycle of motion. Three cycles of motion were computed to obtain a periodic solution. Instantaneous pressure distributions at eight

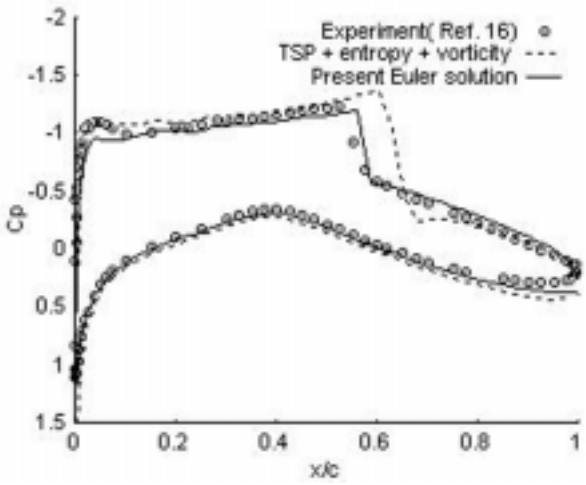

Fig.3 Comparison of steady pressure distributions for RAE 2822 airfoil at M = 0.729 and $\alpha_0 = 2.31°$

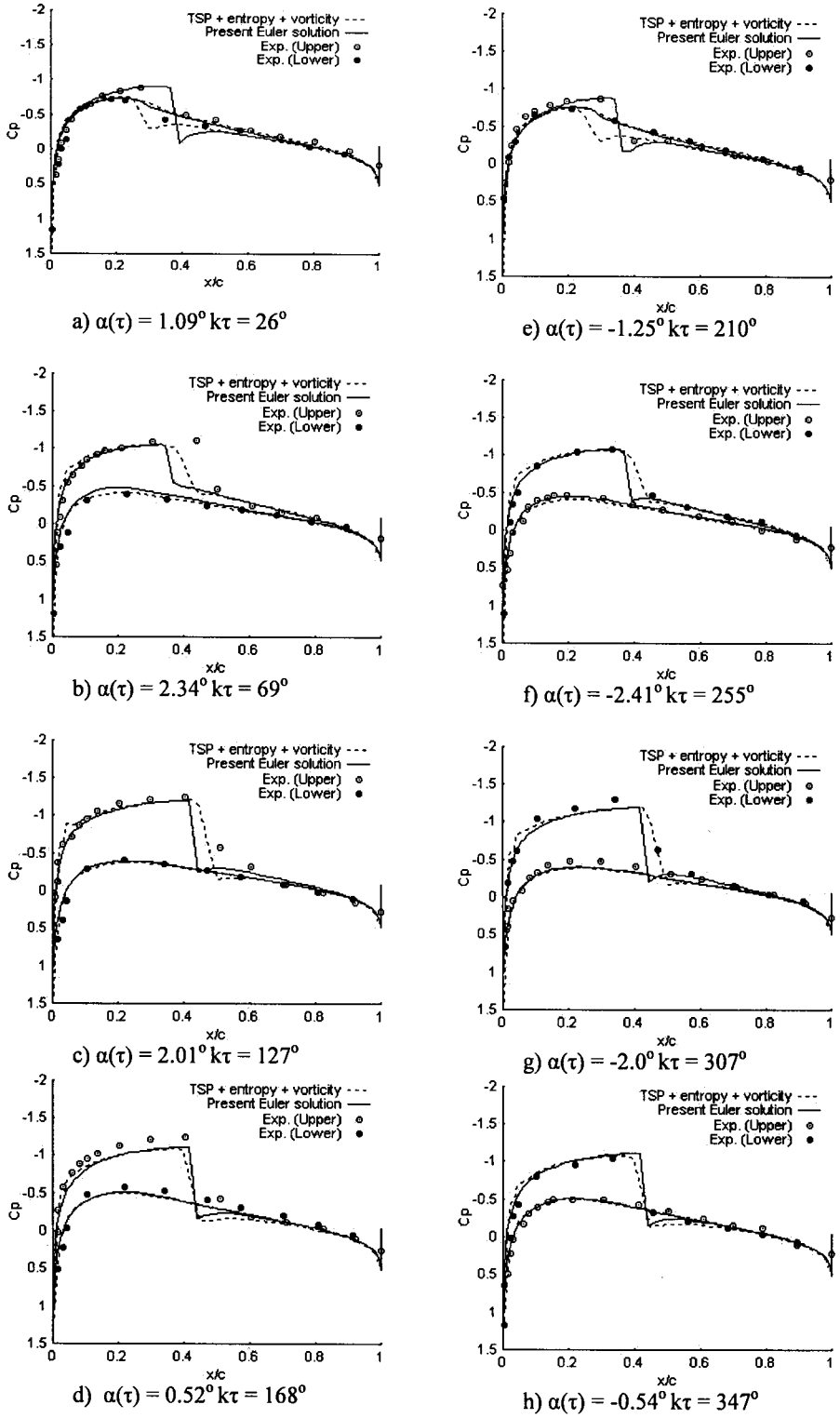

Fig.4 Comparisons of unsteady instantaneous pressure distributions for the NACA 0012 airfoil at M = 0.755, α_0 = 0.016°, α_1 = 2.51° and k = 0.0814

points in time during the third cycle of motion are presented in Fig 4. During the first part of the cycle, there is shock wave on the upper surface of the airfoil and the flow about the lower surface is predominantly sub-critical. During the latter part of the cycle, the flow about the upper surface is sub-critical, and a shock forms along the lower surface. The calculated pressure distributions from the modified TSP code indicate that the shocks oscillate over approximately 25% the chord at different points in time, in general compare well with the experimental data and the comparison is similar to Euler calculation. The modified TSP code captures the shocks sharply and has no difficulty in treating these large shock motions. Comparison of calculated and experimental unsteady lift coefficient verses the instantaneous incidence is shown in Fig 5. Similar observations are noticed in comparing the moment hysteresis curves.

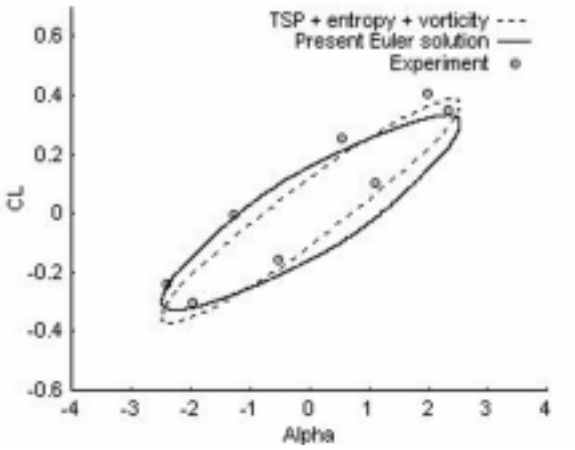

Fig.5 Comparisons of coefficient of lifts vs instantaneous angle of attack for NACA 0012 airfoil pitching at M = 0.755, α_0 = 0.016°, α_1 = 2.51° and k = 0.0814

To assess further, the modified TSP code for unsteady applications, pressures calculated for the NACA 0012 airfoil pitching harmonically about the quarter-chord at M= 0.599 and α_0 = 4.68°. The amplitude of the motion was selected as α_1 = 2.44° and the reduced frequency as k = 0.081 for comparison with the experimental data [13]. The results obtained using 360 steps per cycle of motion, and three cycles for a periodic solution are presented in Fig 6. Results are in good agreement with the experimental data.

Conclusions

Two algorithms developed for unsteady calculations are : Euler code based on finite volume method, cell-centered upwind flux-vector splitting scheme that is naturally dissipative and capture shock wave sharply, using structured computational dynamic mesh, and took special care of time accuracy by applying the implicit version of Euler code. Also modified algorithm for the transonic flow has been developed where, modifications to unsteady transonic small-disturbance theory to include entropy and vorticity effects are presented. The modifications have been implemented in the TSP code, using Approximate Factorization algorithm consisting of Newton linearization technique, which was developed by Singh and Saha [5] Entropy and vorticity effects have been incorporated within the solution procedure to treat cases with strong

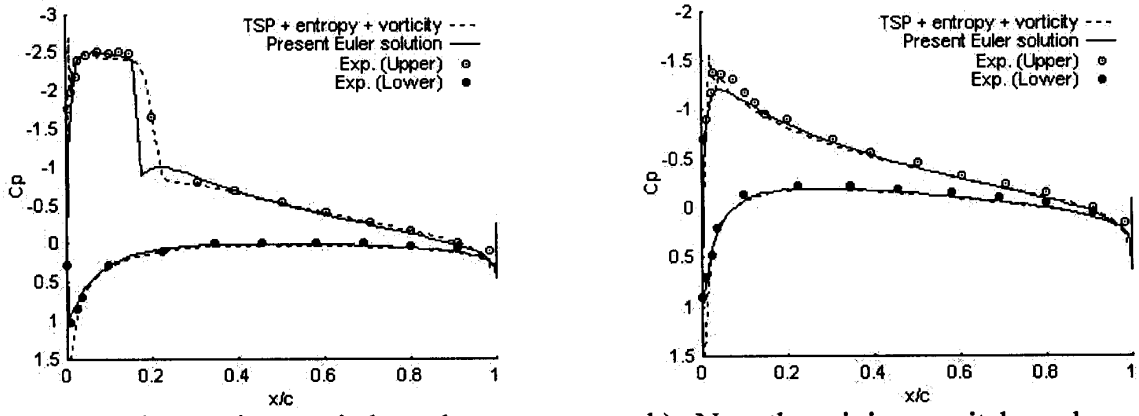

Fig.6 Comparison of instantaneous pressure distributions for the NACA 0012 airfoil at M = 0.599, α_0 = 4.86°, α_1 = 2.44° and k = 0.081

shock waves more accurately. The modified TSP code includes these effects while retaining the relative simplicity and cost efficient of the TSP formulation. For Example, the entropy and vorticity correction do not require any user-selected parameter values, and the increase in CPU time is only approximately 25%.

Steady and unsteady results are presented for the NACA 0012 and the RAE 2822 transonic airfoil to demonstrate applicability of the developed algorithms. Comparisons are made with present Euler solver and with experimental data to assess the accuracy of the code. For the NACA 0012 airfoil, steady pressure computed using the modified theory is in good agreement with the Euler calculations. For cases involving strong shock waves, entropy and vorticity corrections results give good agreement with the Euler solution and with experimental data. Therefore, the present method provides the aeroelastician with an affordable capability to analyze relatively difficult transonic flows without having to solve the computationally more expensive Euler equations.

References

1. Edwards, J. W. and Thomos, J. L., "Computational Methods for Unsteady Transonic Flows", AIAA Paper 87-0107, January 1987.

2. Steinhoff, J. and Jameson, A., "Multiple Solutions of the Transonic Potential Flow Equation", AIAA Paper 81-1019, June 1981.

3. Ballhaus, W. F. and Goorjian, P. M., "Implicit Finite Difference Computations of Unsteady Transonic Flows about Airfoils", AIAA Journal, Vol. 15, No. 12, December 1977, pp. 1728-1735.

4. Batina, J. T., "An Efficient Algorithm for Solution of the Unsteady Transonic Small-Disturbance Equation", Journal of Aircraft, Vol. 25, No. 7, July 1988, pp.598-605.

5. Singh, N. and Saha, S., "Unsteady Transonic Computations for Arbitrary Wing Platforms Using the Transonic Small Disturbance Equation", The Aeronautical Journal of the Royal Aeronautical Society, Aug/Sep 1994. pp. 251-259.

6. Fuglsang, D.F. and Williams, M. H., "Non-Isentropic Unsteady Transonic Small Disturbance Theory", AIAA Paper 85-0600, April 1985.

7. Gibbons, M.D. Whitlow, W, Jr. and Williams, M.H., "Non-isentropic Unsteady Three Dimensional Small Disturbance Potential Theory", AIAA Paper 86-0863, May 1986.

8. Dang, T.Q. and Chen, L.T., "An Euler Correction Method for Two and Three Dimensional Transonic Flows", AIAA Paper 87-0522, January 1987.

9. Hafez, M. and Lovell, D., "Entropy and Vorticity Corrections for Transonic Flows", AIAA Paper 83-1926, July 1983.

10. John T. Batina., "Unsteady Transonic Small-Disturbance Theory Including Entropy and Vorticity Effects", Journal of Aircraft, Vol. 26, No. 6, June 1989.

11. Van Leer, B., "Flux Vector Splitting for the Euler Equations", Lecture Notes in Physics, pp. 507-512, July 1982.

12. Batina, J. T., Implicit Flux-split Euler Schemes for Unsteady Aerodynamics Analysis Involving Unstructured Dynamics Meshes", AIAA Journal,1991, 29, (11), pp.1836-1843.

13. Landon, R.H., "NACA 0012 Oscillating and Transient Pitching, Compendium of Unsteady Aerodynamic Measurements", Data Set 3, AGARD-R-70 August 1982.

14. Thomos, J.L. and Salas, M.D., Far-field Boundary Conditions for Transonic Lifting Solutions to the Euler Equations", AIAA Journal, 1986, 24,(11) pp. 1074-1080.

15. Jameson. A., Schmidt, W. and Turkel, E., "Numerical Solution of the Euler equations by Finite Volume Methods Using Runge-Kutta Time-Stepping Schemes", AIAA Paper 81-1259, AIAA 14th Fluid and Plasma Dynamic Conference, Palo Alto, June 1981.

16. Cook, P.H., McDonald, M.A. and Firmin, M.C.P., "Aerofoil RAE 2822 - Pressure Distributions, and Boundary Layer and Wake Measurements", Experimental Data Base for Computer Program Assessment, AGARD Report AR 138, 1979.